Int. J. Heat Mass Transfer. Vol. 27, No. 5, pp. 781–791, 1984
Printed in Great Britain

0017-9310/84 $3.00 + 0.00
Pergamon Press Ltd.

TECHNICAL NOTES

THE BEHAVIOR OF A WATER DROPLET ON HEATED SURFACES

KUNIHIDE MAKINO
Department of Mechanical Engineering, Maizuru Technical College, Maizuru, Kyoto, Japan

and

ITARU MICHIYOSHI
Department of Nuclear Engineering, Kyoto University, Kyoto, Japan

(*Received* 17 *December* 1982 *and in revised form* 28 *March* 1983)

NOMENCLATURE

- c specific heat of surface material [J kg^{-1} K^{-1}]
- D_0 initial diameter of droplet [m]
- q_t time-averaged heat flux in the contact period [W m^{-2}]
- q_x heat flux at the surface of the semi-infinite solid [W m^{-2}]
- r_t instantaneous base radius of the droplet in contact with the surface [m]
- R radius of droplet [m]
- t time [s]
- T_s saturation temperature [°C]
- T_w instantaneous surface temperature just beneath the droplet [°C]
- T_{w0} initial surface temperature [°C]
- T_{wt} time-averaged surface temperature in the contact period [°C]
- x perpendicular distance from the surface of the solid [m]
- X thermophysical factor of surface material, $\sqrt{(c\rho\lambda/\pi)}$ [J K^{-1} m^{-2} s$^{-1/2}$].

Greek symbols

- θ_0 $T_{w0}-T_s$ [K]
- θ_t $T_{wt}-T_s$ [K]
- $\Delta\theta$ temperature change at the surface [K]
- κ thermal diffusivity of surface material [m^2 s^{-1}]
- λ thermal conductivity of surface material [W m^{-1} K^{-1}]
- ρ density of surface material [kg m^{-3}]
- ρ_l density of pure water [kg m^{-3}]
- σ surface tension of pure water [N m^{-1}]
- τ total evaporation time [s]
- τ_b waiting period [s]
- τ_r first-order vibration period of droplet [s]
- τ_t contact period [s].

1. INTRODUCTION

WHEN a droplet is placed on a heated surface, the liquid comes into direct contact with the solid surface. The first bubbling is delayed, and it is followed by successive boiling in the contact period during which time the droplet keeps in contact with the surface. The length of time from the beginning to the onset of the first bubbling is called the waiting period. On the other hand, the surface temperature, T_w, just beneath the droplet drops suddenly from the initial temperature, T_{w0}, by direct contact and thereafter is kept at a nearly constant temperature, near T_{wt}, in the contact period [1]. Though the initial surface temperature is comparatively high, the droplet makes contact first, and then bounces or floats. This behavior of the droplet is reported in refs. [2–5].

As to the contact period, τ_t, of a droplet for T_{w0} either near or above the Leidenfrost point, Wachters *et al.* [6] studied τ_t with a high-speed camera and Nishio and Hirata [2, 7] with an electro-probe as well as boiling sounds. Their results show that in the foregoing temperature range τ_t is independent of T_{w0} being nearly equal to τ_r, which is the first-order vibration period of a spherical droplet derived by Rayleigh [8]. Unfortunately there are no systematic experiments on the waiting period, τ_b, except those of Nishio and Hirata [2], who used a quartz-prism as a heated surface in the very high temperature range (> 430°C). Other works using a stainless steel surface showed only the transient surface temperature [3–5], but τ_b can be found from their experimental data. The behavior of impinging drops in the contact period was studied by Wachters and Westerling [9] and Ueda *et al.* [10]. While photographing the impact of a water drop upon a quartz surface at a temperature above the Leidenfrost temperature, Groendes and Mesler [11] measured the transient surface temperature. The data with relation to the differences in the two temperatures, T_{w0} and T_{wt}, are few and the two temperatures can be seen merely from the transient surface temperature reported in refs. [3–5] for a stainless steel surface.

In order to clarify the transient heat transfer in the contact period, it is inevitable to get the systematic information about the behavior of a droplet. This note presents mainly the behavior of a water droplet in contact with a heated surface of which the initial temperature is above the atmospheric saturation temperature of water, and the final temperature is greater than the Leidenfrost temperature. The behavior of the droplet is observed by high-speed photography, from which both the contact and the waiting periods are derived. Some relationships between the two temperatures, T_{w0} and T_{wt}, as well as the time-averaged heat flux, q_t, in the contact period are also obtained from experimental data. A part of this note is devoted to a discussion of the heat transfer characteristics in the contact period.

2. THE BEHAVIOR OF A DROPLET

2.1. *Contact period*

2.1.1. *Experimental apparatus and procedure.* Water droplets with diameters of 2.54, 3.29 and 4.50 mm and heated plates of four kinds of materials (copper, brass, carbon steel and stainless steel) were used. These plates were of the same size (150 mm diameter and 20 mm thick) and slightly concaved, so that droplets did not spill off. The same surface treatments and setting procedure of an initial surface temperature were adopted as in refs. [1, 12].

If a droplet comes into contact with the surface, the electric

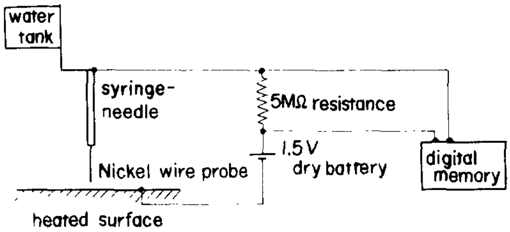

FIG. 1. Schematical diagram of the experimental apparatus with an electro-probe.

resistance between the droplet and the surface is reduced, and this can also be noticed by the appearance of the droplet and the change in the surface temperature just beneath the droplet. These three methods are used for detecting the contact period.

The experimental apparatus using an electro-probe is shown in Fig. 1. The probe, a bare nickel wire, 0.2 mm diameter, is set inside the syringe-needle used for placing the droplet, and is held about 0.1 mm above the heated surface. When a droplet touches the tip of the probe and the surface, a close circuit using a resistance of 5 MΩ and a 1.5 V dry battery is completed. The change in the voltage between the terminals of the resistance can be measured by a digital memory device. The contact period may be displayed by a pen recorder or a synchroscope. Figures 2(a) and (b) show examples of the changes in voltage for the case of a 3.29 mm diameter droplet on a stainless steel plate at $T_{w0} = 330$ and 240°C, respectively. According to the time scales, the contact period τ_t can be seen as 16 ms and 0.14 s for Figs. 2(a) and (b), respectively.

If a droplet is placed between an illuminating lamp and a high-speed camera, the shadow of the droplet can be photographed. Two examples are shown for the case of a 3.29 mm diameter droplet on a stainless steel plate at $T_{w0} = 359$ and 250°C in Figs. 3(a) and (b), respectively. The tip of the syringe-needle is seen in the upper center, and the real as well as the inverted image of the droplet can be seen in each photograph (due to the mirror-finished treatment of the surface). The contact period, τ_t, can be determined from the contact duration of the two images on a series of photographs, in which the lapses of time are labelled by measured time marks of 1000 Hz on the edge of the high-speed film; in Figs. 3(a) and (b) $\tau_t = 25$ and 85 ms, respectively.

The change in surface temperature, T_w, measured in the previous paper [1], with a sheathed chromel–alumel thermocouple soldered on the surface, can be used for the estimation of the contact period. The examples of the change in T_w are shown in Figs. 4(a) and (b) for the case of a stainless steel plate and $D_0 = 3.29$ mm at $T_{w0} = 310$ and 240°C, respectively. Points ① and ② on Figs. 4(a) and (b) are the moments of touch and detouch, respectively. The time-interval of these points is the contact period τ_t; 28 and 110 ms in Figs. 4(a) and (b), respectively. At point ③ in Fig. 4(a), some split bouncing droplets might retouch the junction of the thermocouple.

However, there are some weaknesses in these detecting methods. A droplet may be hung over by the electro-probe wire. Generally the contact of the two images on a series of the photographs does not mean the direct contact of the droplet with the surface. But even if the vapor layer exists between the droplet and the surface, the two images appear to be in contact with each other according to the photographs. The solder used for fastening the thermocouple to the heated surface may affect the wettability of a droplet and also the temperature indicated by the thermocouple can be influenced by a time-constant of the thermocouple in a short contact period.

2.1.2. *Results and discussion.* Figure 5 shows examples of the results of τ_t obtained by these three methods together with the method of using a stop watch to measure the total evaporation time, τ, in the wide temperature range which includes the nucleate boiling, the transition boiling and the film boiling regions classified in previous papers [1, 12]. The case for a 3.29 mm diameter droplet on a stainless steel surface is shown in Fig. 5. In the nucleate boiling region ($T_{w0} < 200$°C), the two periods, τ_t and τ, might be the same. The data of τ_t seem to be correlated by a curve. The effect of the thermophysical factor* of the surface material will be described later.

The effects of the initial diameter, D_0, of the droplet on the contact period, τ_t, are shown in Figs. 6(a) and (b). Figure 6(a) shows that, except for the high temperature range, the relation between τ_t and θ_0 for each D_0 gives a straight line in logarithmic scales, and these lines are parallel to each other, thus τ_t is a function of the power forms of θ_0. In the high temperature range, τ_t might be equal to τ_r as pointed out by Wachters *et al.* [6] and Nishio and Hirata [2, 7]. The first-order vibration period, τ_r, of a freely oscillating droplet is expressed as [8]

$$\tau_r = \pi\sqrt{[(\rho_1 R^3)/(2\sigma)]}. \quad (1)$$

We can calculate the constant values of τ_r for each D_0, which are shown on Figs. 5 and 6(a). The contact periods, τ_t, might be proportional to $R^{3/2}$ or $D_0^{3/2}$ in the same way as τ_r in equation (1). Using this idea and the same data as in Fig. 6(a), we can get a

* When the surface temperature of a semi-infinite solid changes stepwisely, the heat flux, q_x, at the surface [13] is

$$q_x = -\lambda(\partial\theta/\partial x)_{x=0} = \lambda\Delta\theta/\sqrt{(\pi\kappa t)}$$
$$= \sqrt{(c\rho\lambda/\pi)}\Delta\theta/\sqrt{t} = \Delta\theta X/\sqrt{t}.$$

Baumeister *et al.* [14] and Wachters *et al.* [15] insist that the value of $c\rho\lambda$ or the inverted one is an important factor in their researches of Leidenfrost phenomena.

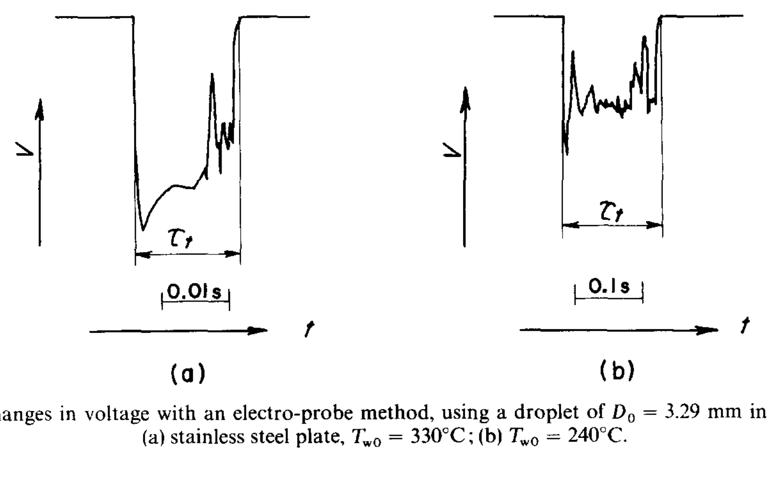

FIG. 2. Changes in voltage with an electro-probe method, using a droplet of $D_0 = 3.29$ mm in diameter: (a) stainless steel plate, $T_{w0} = 330$°C; (b) $T_{w0} = 240$°C.

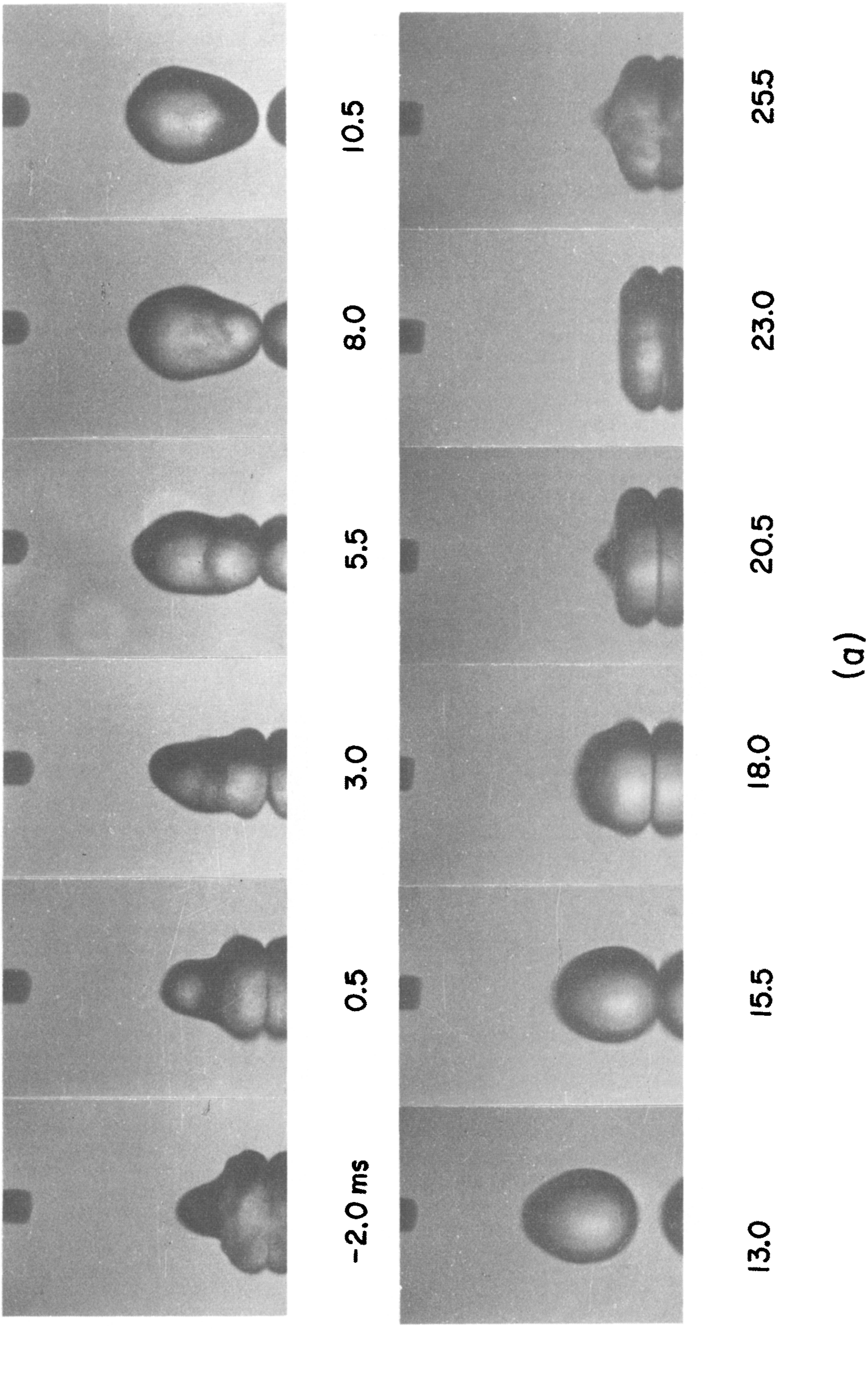

FIG. 3. Photographs of an evaporating droplet of $D_0 = 3.29$ mm on a stainless steel plate taken by a high-speed camera: (a) $T_{wo} = 359°C$; (b) $T_{wo} = 250°C$.

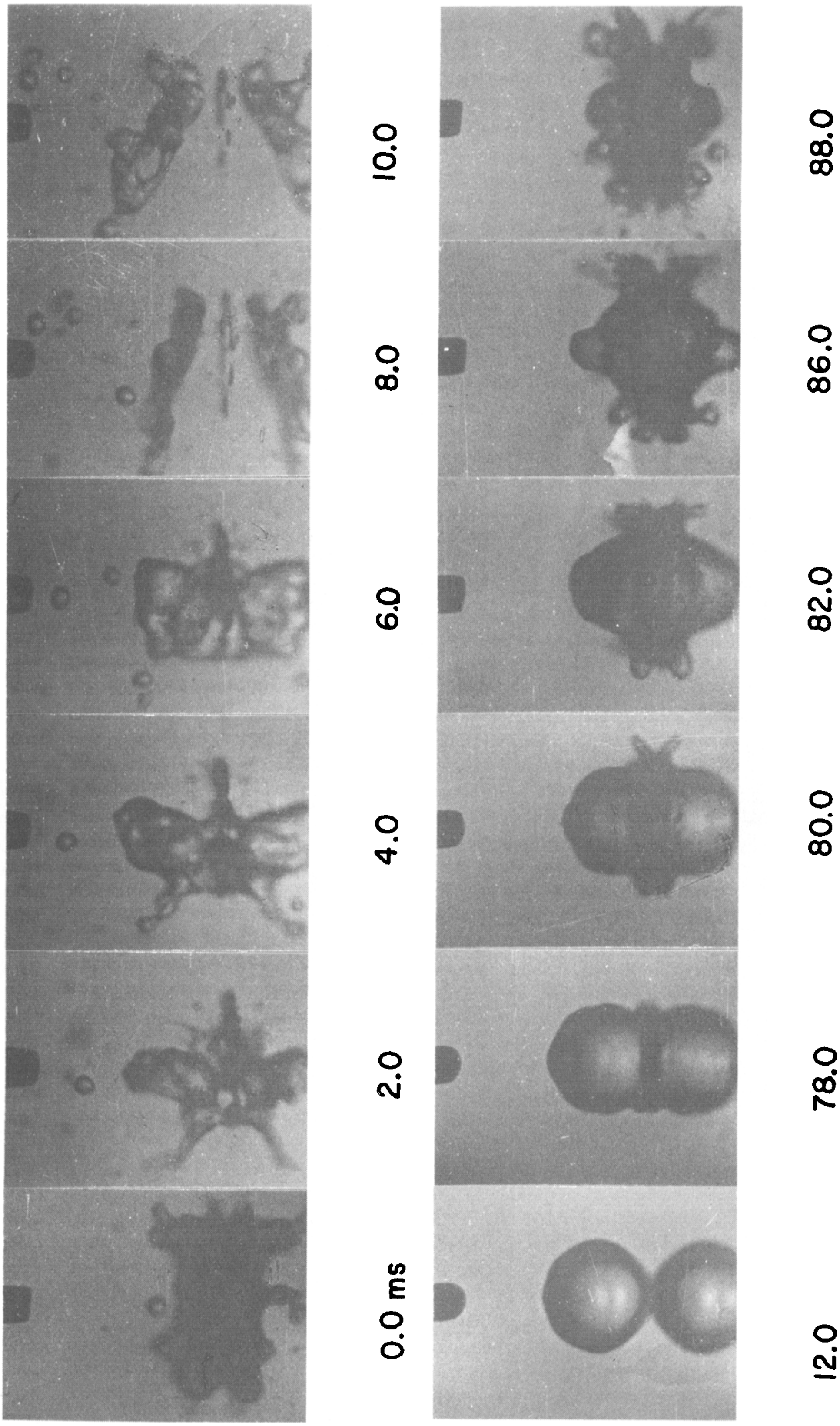

FIG. 3(b).

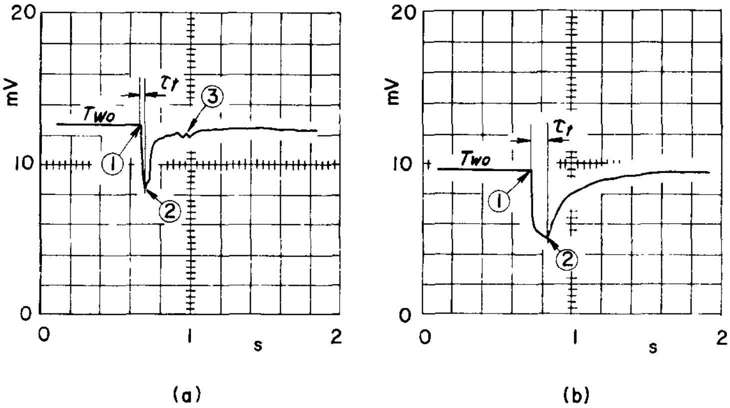

FIG. 4. Changes in e.m.f. of T_w-thermocouple of stainless steel plate: (a) T_{w0} = 310°C; (b) T_{w0} = 240°C.

straight line which correlates well to the data for any D_0 as shown in Fig. 6(b).

If we take into consideration the thermophysical factor X, the contact period may be expressed as

$$\tau_t = c_1 X^1 D_0^{3/2} \theta_0^m. \tag{2}$$

Using about 800 pieces of experimental data obtained for four various kinds of surface materials and least squares, the following empirical equation is obtained

$$\tau_t = 1.51 \times 10^{17} X^{-2.20} D_0^{3/2} \theta_0^{-3.01}, \tag{3}$$

which is shown in Figs. 5 and 6(a) and (b). The intersection of equations (1) and (3) might be recognized as a Leidenfrost point. For a higher surface temperature range than the Leidenfrost point, τ_t is slightly longer than τ_r given by equation (1). We call the droplet placed on the higher surface temperature range the Leidenfrost droplet.

2.2. *Waiting period*

2.2.1. *Experimental apparatus and procedure.* The waiting period is observed by using a high-speed camera at 500–1000 frames per second.

2.2.2. *Results and discussion.* Figures 7(a)–(c) show examples of photographs in which a 3.29 mm diameter droplet is used. Figure 7(a) shows the appearance of a droplet on a brass plate at T_{w0} = 170°C, Fig. 7(b) on a carbon steel plate at T_{w0} = 230°C, and Fig. 7(c) on a carbon steel plate at T_{w0} = 260°C.

Lesser [16] analyzed theoretically the diffusion of a shock

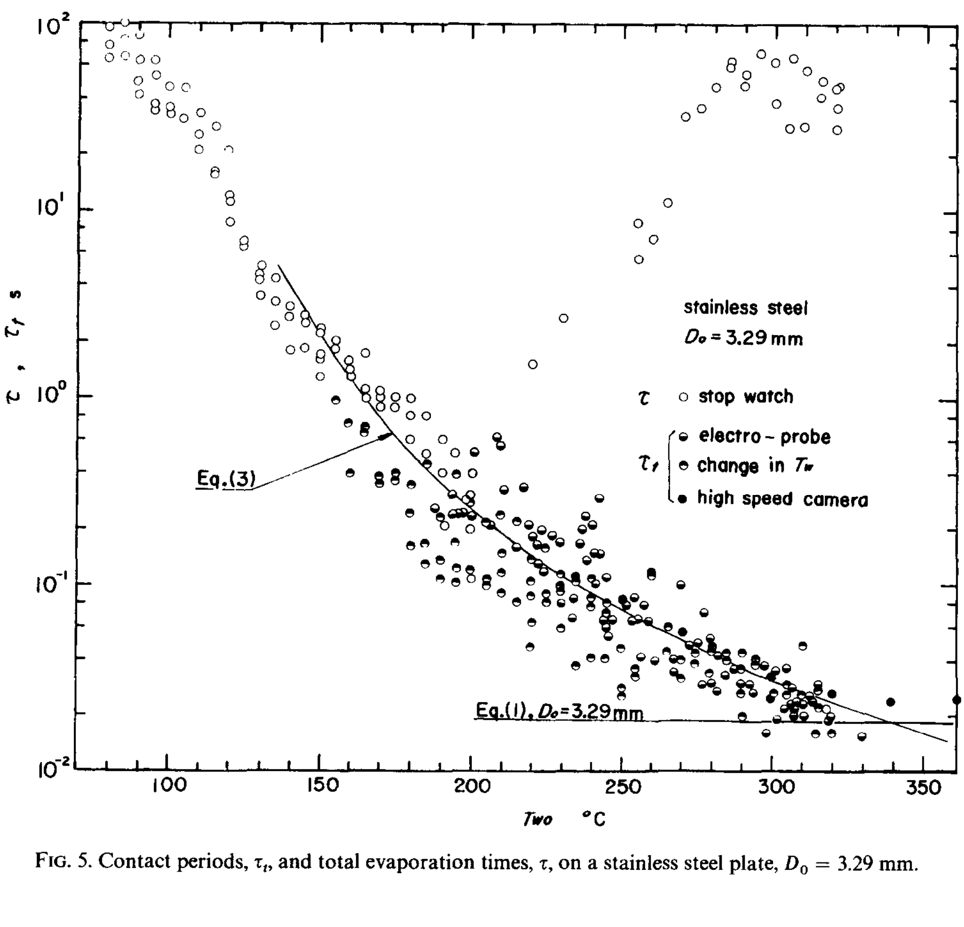

FIG. 5. Contact periods, τ_t, and total evaporation times, τ, on a stainless steel plate, D_0 = 3.29 mm.

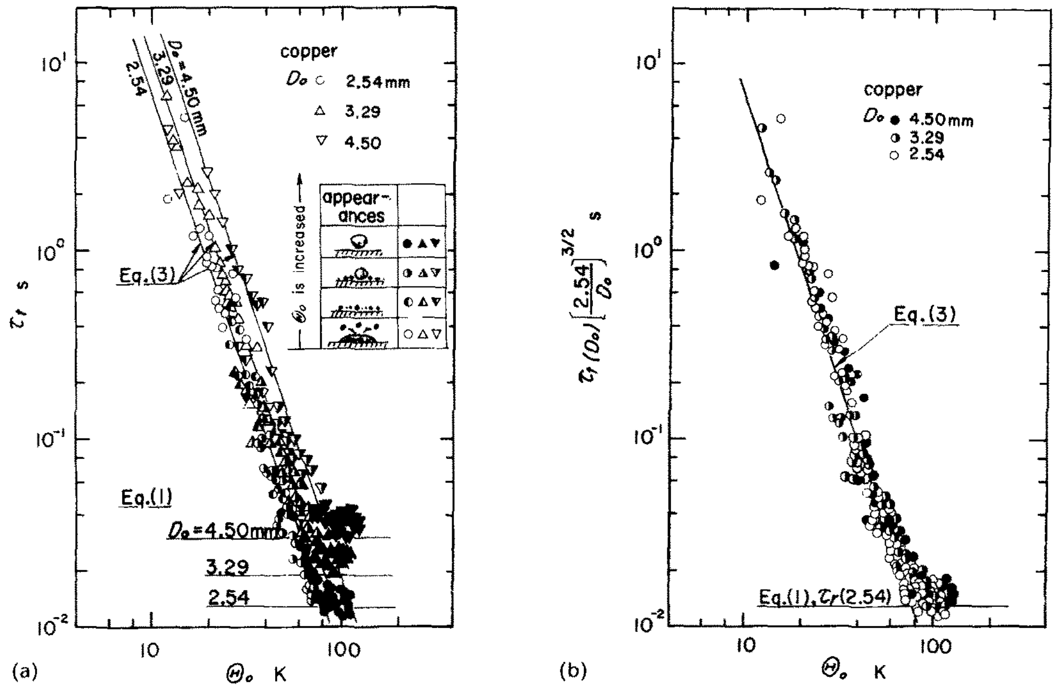

FIG. 6. Contact periods, τ_t: (a) effects of initial diameter of droplet; (b) rearrangement of contact periods τ_t.

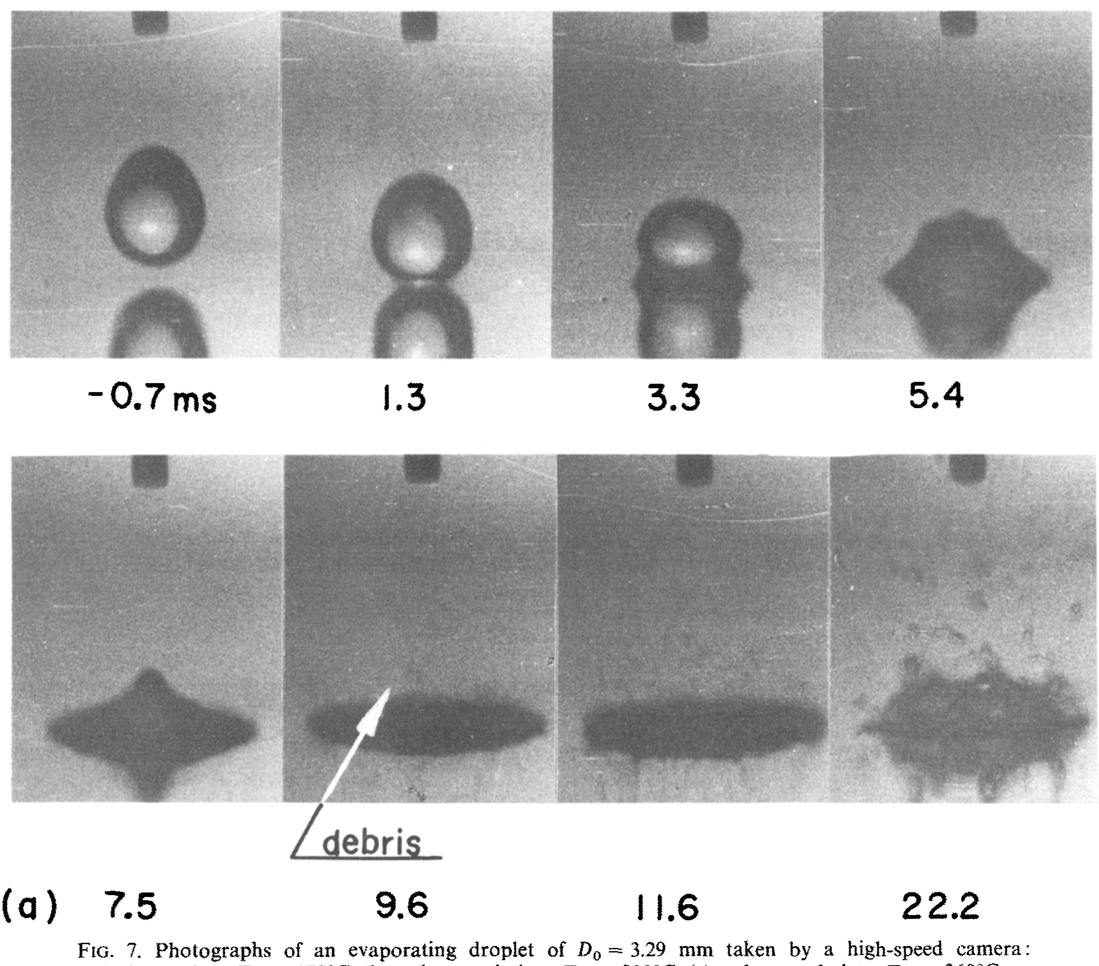

FIG. 7. Photographs of an evaporating droplet of $D_0 = 3.29$ mm taken by a high-speed camera: (a) brass plate, $T_{wo} = 170°C$; (b) carbon steel plate, $T_{wo} = 230°C$; (c) carbon steel plate, $T_{wo} = 260°C$.

wave within a drop striking against an unheated solid. He explained that when the spreading speed of the edge of a drop on the solid surface was slower than the sonic speed in the drop, the edge was disturbed constantly by the sonic speed shock wave, thereby the drop could spread on the unheated surface at an acute angle at the edge. A numerical solution based on a three-dimensional unsteady model of the dropwise evaporation on a heated plate by Rizza [17] indicated that a large portion of heat was transferred through the droplet at the edge. Accordingly, a considerable concentration of heat flux at the edge may initiate the first bubbling during the spreading process. After the bubbling occurs at the edge, the vapor generated between the droplet and the heated surface may disturb the edge. Thus the angle of the edge changes from an acute angle into an obtuse one and the edge can possibly be turned up.

The vapor flow between a droplet and a heated surface of both solids and liquids was studied by Wachters *et al.* [6] and Iida and Takashima [18], respectively. Iida and Takashima [18] said that the vapor flow was laminar and its Reynolds number was about 90. So the turned up edge can not be blown away by the vapor flow.

In Fig. 7(a) the angle of the edge is acute even after 11.6 ms have lapsed. This means that the bubbling has not yet occurred at the edge. But the photograph at 9.6 ms shows some very small debris above the droplet. The debris might be yielded from the bubbling at the bottom of the droplet. In this case vapor flows through the spreading droplet, not between the droplet and the surface, from the point of view of flowing resistance of the vapor. Time marks on the high-speed film indicate that the waiting period, τ_b, is about 9.0 ms. In Fig. 7(b) the appearance at 4.5 ms has presented a considerable obtuse angle already. The waiting period, τ_b, is assumed to be 3.0 ms. In Fig. 7(c), the waiting period, τ_b, is shorter than in both Figs. 7(a) and (b), and is about 2.0 ms.

The waiting period, τ_b, has been estimated mainly by the generation of the very small debris above the spreading droplet in the low temperature range and by the consideration of the angle of the edge in the high temperature range.

It is easy to determine the base radius, r_t, of the droplet in contact with the surface at any time using the series of photographs in Figs. 7(a)–(c) and 3(a) and (b), if we assume the droplet base to be circular. Examples of the results are shown in Figs. 8 and 9. Figure 8 shows the effects of T_{w0} on r_t for $D_0 = 3.29$ mm and a carbon steel plate. Figure 9 also shows the effects of D_0 on r_t for a stainless steel plate at $T_{w0} = 360°C$. In these figures $\times$ and $\uparrow$ designate the waiting period and $\tau_r/2$, respectively. It is difficult to measure precisely intervals shorter than 1 ms by means of 1000 Hz time marks on the film. This is the reason why $\times$'s cannot be seen in Fig. 9.

The higher the initial surface temperature T_{w0} is, the shorter the waiting period τ_b becomes. The gradient dr_t/dt and the value of r_t are kept nearly constant in the waiting period regardless of the surface material and the initial diameter of the droplet. In the higher temperature range r_t exhibits a maximum value at about $\tau_r/2$. The half period of τ_r is the period in which the shape of a droplet changes from an initial spherical state into a flat ellipsoid. This is independent of T_{w0} for the Leidenfrost droplet. The maximum value of r_t tends to decrease as T_{w0} increases, and this fact means that since

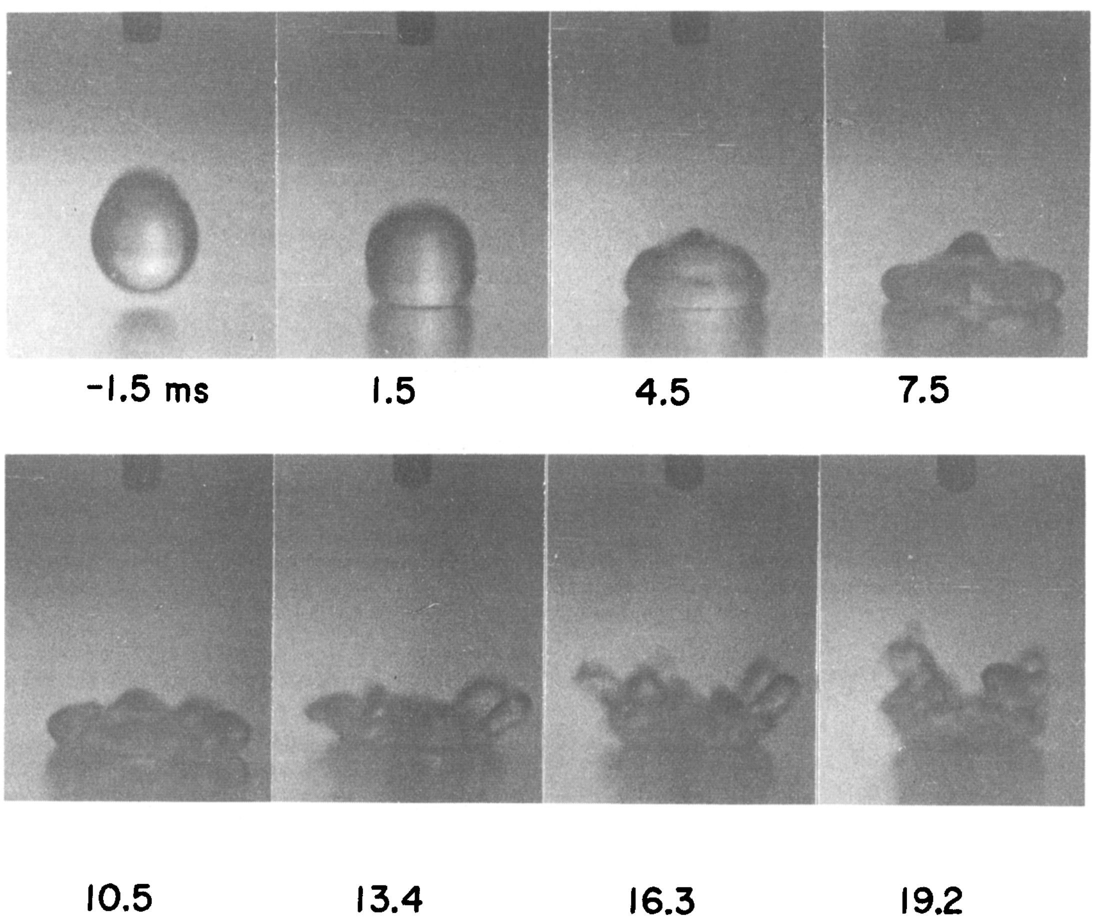

FIG. 7(b).

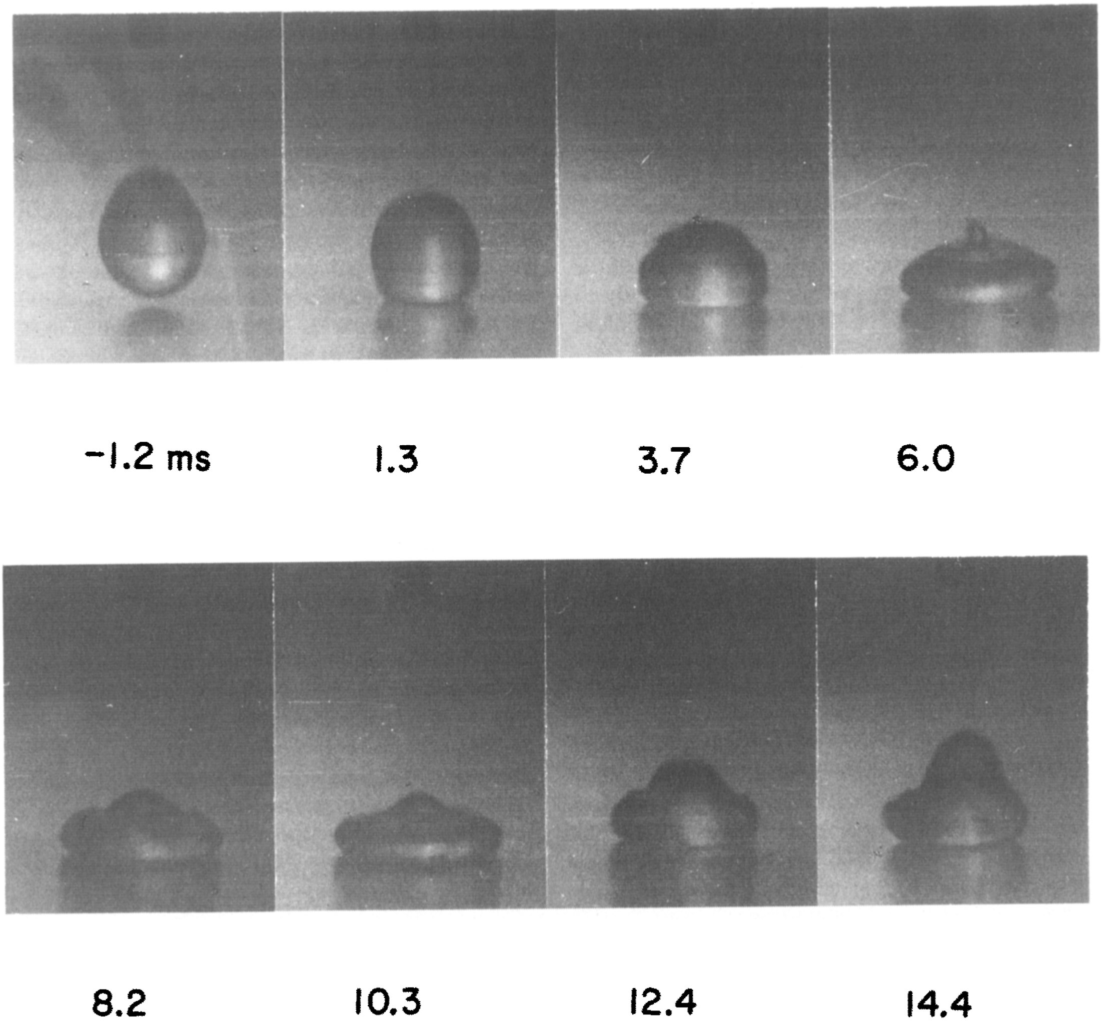

FIG. 7(c).

the generated vapor on the surface impedes the spreading of the droplet, the shorter the waiting period, the greater the impedance. This results in a decrease of the maximum value of r_t.

The summary relations between r_t and t for about 80 pieces of data in the waiting period are collected within the hatched zone in Fig. 10. We can obtained an equation showing the relation between them in the waiting period regardless of D_0 and X

$$r_t = 3.16\times 10^{-2} t^{1/2}, \quad 0 \leqslant t \leqslant \tau_b. \tag{4}$$

This relation is shown in Fig. 10.

Figure 11 presents the results of the waiting period, where the relation of τ_b vs θ_0 seems to give a straight line for each surface material regardless of D_0. If we assume that τ_b is a

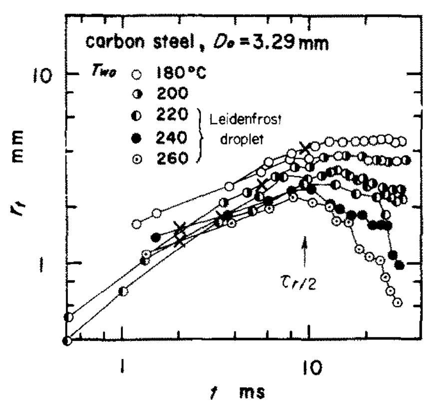

FIG. 8. Effects of initial surface temperature on the base radius, r_t, for a droplet of $D_0 = 3.29$ mm and a carbon steel plate.

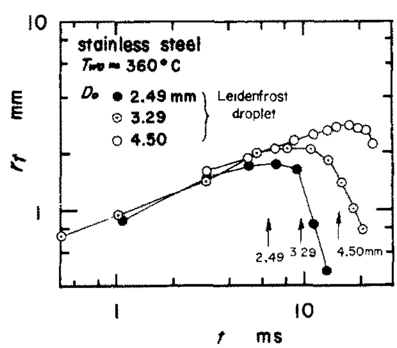

FIG. 9. Effects of D_0 on the base radius, r_t, for a stainless steel plate, $T_{wo} = 360$°C.

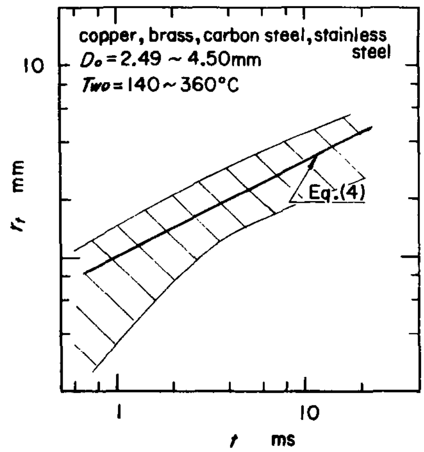

FIG. 10. Summary relation between r_t and t of a droplet of $D_0 = 2.49$–4.50 mm, on four kinds of surface materials, $T_{w0} = 140$–360°C.

function of power forms of θ_0 and X, we can obtain the following empirical correlation

$$\tau_b = 4.67\times10^{12}X^{-2.13}\theta_0^{-3.35}. \tag{5}$$

The relation is illustrated for each surface material on Fig. 11.

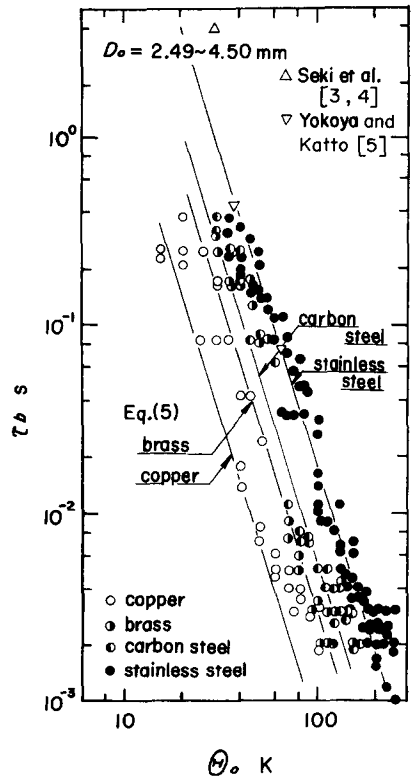

FIG. 11. Waiting periods, τ_b, for four kinds of surface materials.

T_{w0} AND T_{wt}

Since the surface temperature T_w just beneath the droplet measured by the sheathed thermocouple varies with time as in Figs. 4(a) and (b) (see also Figs. 7 and 8 in ref. [1]), we can deal with the time-averaged surface temperature, T_{wt}, in the contact period. An example of the relation between T_{wt} and T_{w0} is shown in Fig. 12 for a stainless steel plate and the various initial diameter, D_0, of the water droplets. It has a linear relation regardless of D_0. This tendency is similar to those of other surface materials. Taking into consideration the thermophysical factor, X, of the surface material, the relation may have the form

$$\theta_0/\theta_t = c_3X^p. \tag{6}$$

However, there are some problems in measuring the changes in T_w. When a droplet does not hit the thermocouple junction for the surface temperature perfectly, the longer the missing distance from the junction is and the higher the thermal diffusivity of the surface material is, the less the change in T_w. Moreover, a thermocouple has a time constant in its response, and T_w is apt to be measured higher. Hence the temperature, T_{wt}, tends to be estimated higher. The data shown in Fig. 12 includes these problems, particularly those of short contact periods or the high temperature range. The lowest data of T_{wt} for each T_{w0} may exhibit the exact values.

After due consideration of these problems the coefficient

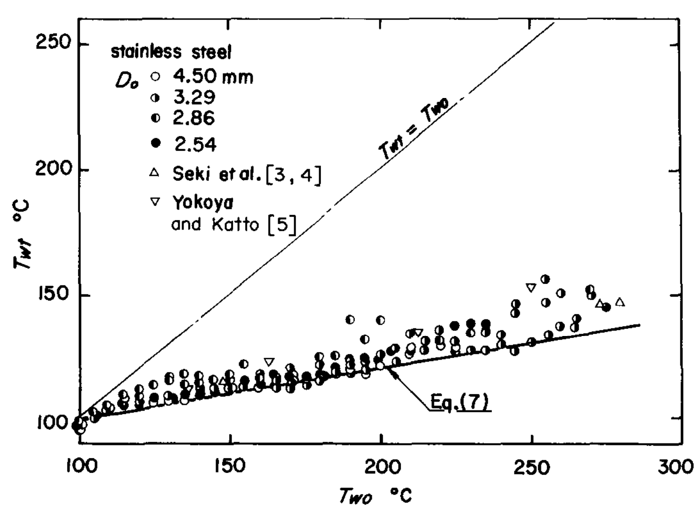

FIG. 12. Relation between T_{wt} and T_{w0} for a stainless steel plate.

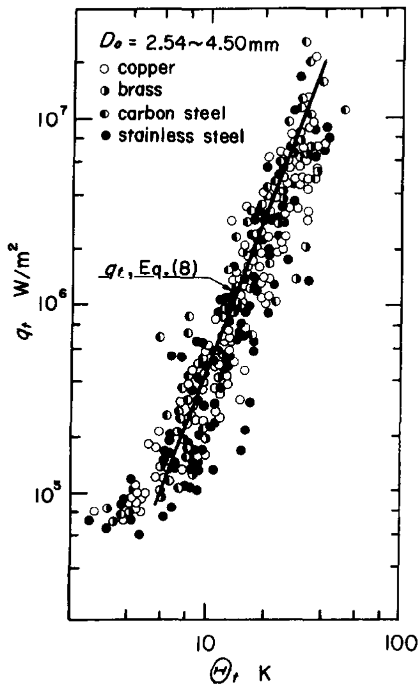

FIG. 13. Time-averaged heat flux, q_t, in the contact period for $D_0 = 2.54$–4.50 mm and various kinds of surface materials.

and the exponent in equation (6) are decided

$$\theta_0 = 2.23 \times 10^3 X^{-0.729} \theta_t. \tag{7}$$

The relation of equation (7) is seen in Fig. 12.

THE RELATION BETWEEN q_t AND θ_t IN THE CONTACT PERIOD

One of the interesting and important points is to investigate the heat transfer characteristics in the contact period. The relationship between q_t and θ_t in the contact period obtained with the droplets of $D_0 = 2.54$–4.50 mm in diameter seem to give a straight line, no matter what material is used for the heated plate and no matter which size of aroplet is used for the initial diameter as shown in Fig. 13. This is true when the nucleate boiling continues after the onset of the first bubbling in the contact period. Using about 400 pieces of experimental data, we obtain

$$q_t = 770 \times \theta_t^{2.78}, \tag{8}$$

although the exponent of θ_t might be larger for a higher q_t because of the aforementioned problems of T_w-measurement. The relation of equation (8) is shown in Fig. 13, and it indicates characteristics of very high heat transfer in the contact period.

It can be seen from Fig. 13 that $q_t \geqslant 6 \times 10^6$ W m^{-2} for $\theta_t \geqslant 25$ K. Even in such a high surface temperature range, since the droplet is in contact with the surface in a short period until it begins to bounce or float, q_t can be correlated with θ_t as shown in Fig. 13, though some difficulties for determining q_t and θ_t arise as the contact period becomes shorter. Thus it might be said that the highest value q_t can reach is about 10^7 W m^{-2} or more in the contact period.

CONCLUSION

By studying experimentally the behavior and the heat transfer characteristics in the contact period of a pure water droplet of $D_0 = 2.54$–4.50 mm in diameter on smooth surfaces of copper, brass, carbon steel and stainless steel, the empirical equations (3)–(5) can be derived for expressing the contact period, τ_t, against D_0, X and θ_0, change in the base radius, r_t, of a droplet with time in the waiting period, and the waiting period, τ_b, against X and θ_0, respectively. An empirical correlation of q_t with θ_t is represented by equation (8) independent of the surface material and initial droplet diameter since θ_t can be expressed by equation (7), and it shows characteristics of very high heat transfer in the contact period.

The highest values of q_t are attainable in the contact period in such a high surface temperature range as that of $\theta_t \geqslant 25$ K and are about 10^7 W m^{-2}, although they can be higher.

REFERENCES

1. I. Michiyoshi and K. Makino, Heat transfer characteristics of evaporation of a liquid droplet on heated surfaces, *Int. J. Heat Mass Transfer* **21**, 605–613 (1978).
2. S. Nishio and M. Hirata, Study on the Leidenfrost temperature—2nd Report, Behavior of liquid–solid contact surface and Leidenfrost temperature, *Trans. Japan Soc. Mech. Engrs* **44** (380), 1335–1346 (1978).
3. M. Seki, H. Kawamura and K. Sanokawa, Unsteady state heat transfer of impinging droplets—1st Report, Measurements of change in temperature of heated surface, in *Proc. 9th National Heat Transfer Symp. of Japan*, pp. 459–462. Heat Transfer Soc. Japan, Hiroshima (1972).
4. M. Seki, H. Kawamura and K. Sanokawa, Transient temperature profile of a hot wall due to an impinging liquid droplet, *Trans. Am. Soc. Mech. Engrs*, Series C, *J. Heat Transfer* **100**, 167–169 (1978).
5. S. Yokoya and Y. Katto, Thermal and contact conditions at the interface when a liquid droplet placed on a solid surface of high temperature, in *Proc. 15th National Heat Transfer Symp. of Japan*, pp. 181–183. Heat Transfer Soc. Japan, Sapporo (1978).
6. L. H. J. Wachters, H. Bonne and H. J. van Nouhuis, The heat transfer from a hot horizontal plate to sessile water drops in the spheroidal state, *Chem. Engng Sci.* **21**, 923–936 (1966).
7. S. Nishio and M. Hirata, Study on the Leidenfrost temperature—1st Report, Experimental study on the fundamental characteristics of the Leidenfrost temperature, *Trans. Japan Soc. Mech. Engrs* **43**(374), 3856–3867 (1977).
8. Lord Rayleigh, On the capillary phenomena of jets, *Proc. R. Soc. Lond.* **XXIX**, 71–97 (1879).
9. L. H. J. Wachters and N. A. J. Westerling, The heat transfer from a hot wall to impinging water drops in the spheroidal state, *Chem. Engng Sci.* **21**, 1047–1056 (1966).
10. T. Ueda, T. Enomoto and M. Kanetsuki, Heat transfer characteristics and dynamic behavior of saturated droplets impinging on a heated vertical surface, in *Proc. 15th National Heat Transfer Symp. of Japan*, pp. 283–285. Heat Transfer Soc. Japan, Sapporo (1978).
11. V. Groendes and R. Mesler, Measurement of transient surface temperature beneath Leidenfrost water drops, *Heat Transfer 1982, Proc. 7th Int. Heat Transfer Conf.*, München, Vol. 4, pp. 131–136. Hemisphere, Washington, DC (1982).
12. K. Makino and I. Michiyoshi, Effects of the initial size of water droplet on its evaporation on heated surfaces, *Int. J. Heat Mass Transfer* **22**, 979–981 (1979).
13. H. S. Carslaw and J. C. Jaeger, *Conduction of Heat in Solids* (2nd edn.). Oxford University Press, Oxford (1959).
14. K. J. Baumeister and F. F. Simon, Leidenfrost temperature—its correlation for liquid metals, cryogens, hydrocarbons, and water, *Trans. Am. Soc. Mech. Engrs*, Series C, *J. Heat Transfer* **95**, 166–172 (1973).
15. L. H. J. Wachters, L. Smulders, J. R. Vermeulen and H. C. Kleiweg, The heat transfer from a hot wall to impinging mist droplets in the spheroidal state, *Chem. Engng Sci.* **21**, 1231–1238 (1966).

16. M. B. Lesser, Analytic solutions of liquid-drop impact problems, *Proc. R. Soc. Lond.* **A377**, 289–308 (1981).
17. J. J. Rizza, A numerical solution to dropwise evaporation, *Trans. Am. Soc. Mech. Engrs*, Series C, *J. Heat Transfer* **103**, 501–507 (1981).
18. Y. Iida and T. Takashima, Evaporation of a liquid drop on a hot liquid surface—2nd Report, Experiment and analysis of Leidenfrost film boiling on a liquid surface, *Trans. Japan Soc. Mech. Engrs* **B48**(430), 1128–1136 (1982).

Int. J. Heat Mass Transfer. Vol. 27, No. 5, pp. 791–794, 1984
Printed in Great Britain
0017–9310/84 $3.00 + 0.00

FREE CONVECTION OF NON-NEWTONIAN FLUIDS OVER NON-ISOTHERMAL TWO-DIMENSIONAL BODIES

A. SOM* and J. L. S. CHEN
Department of Mechanical Engineering, University of Pittsburgh, Pittsburgh, PA 15261, U.S.A.

(*Received* 15 *November* 1982 *and in revised form* 9 *June* 1983)

INTRODUCTION

HEAT transfer in non-Newtonian fluids is of practical importance in many industries, for example in paper making, drilling of petroleum products, slurry transporting, and processing of food and polymer solutions.

Acrivos [1] was apparently the first to investigate in 1960 the natural convection behavior of non-Newtonian fluid flow from a body with an isothermal surface. Since then quite a number of investigations have been done with success [2–12]. An excellent review on the subject of convective heat transfer in non-Newtonian fluids has recently been made by Shenoy and Mashelkar [13].

Most of the studies on free convection in non-Newtonian fluids are concerned with simple bodies such as a flat plate or cylinder with uniform wall temperature or uniform surface heat flux. In a great many technical applications, however, the body shape is neither flat nor cylindrical and its surface is thermally non-uniform, on which attention will be focused here. In considering such problems, it is natural to examine the family of bodies having certain wall-temperature or wall-flux variations which will give rise to similarity thermal characteristics.

The objective of this work is to analyze the free convection heat transfer in power-law non-Newtonian fluids from a two-dimensional (2-D) body of which the surface is subject to power-law variations in (a) temperature and (b) heat flux. In view of the fact that most of the non-Newtonian fluids have large Prandtl numbers, this study is directed towards such fluids. Similar temperature profiles and heat transfer results are presented, also examined in detail are the effects of body shape, flow index, and surface thermal variations.

ANALYSIS

Consider a 2-D body submersed in a quiescent bulk of power-law non-Newtonian fluid at constant temperature T_∞. The boundary-layer equations of free convection in the steady, laminar, and incompressible flow are

$$\frac{\partial u}{\partial x}+\frac{\partial v}{\partial y}=0, \tag{1}$$

$$u\frac{\partial u}{\partial x}+v\frac{\partial u}{\partial y}=g_x\beta(T-T_\infty)+\frac{K}{\rho}\frac{\partial}{\partial y}\left[\left|\frac{\partial u}{\partial y}\right|^{n-1}\frac{\partial u}{\partial y}\right], \tag{2}$$

$$u\frac{\partial T}{\partial x}+v\frac{\partial T}{\partial y}=\alpha\frac{\partial^2 T}{\partial y^2}, \tag{3}$$

where (x, y) are curvilinear coordinates with x measured from the front stagnation and along the body contour; (u, v) are velocity components in these directions; T is the temperature; ρ, the fluid density; α, the fluid thermal diffusivity; β, the thermal expansion coefficient; and K and n are the fluid consistency and flow index of the power-law fluid, respectively. The x-component of gravitational acceleration, g_x, is related to the body-contour angle, ε, by $g_x = g \sin\varepsilon$, in which ε is the angle between the y- and g-axis and is given by

$$\varepsilon=\sin^{-1}\left[1-\left(\frac{\mathrm{d}R}{\mathrm{d}x}\right)^2\right], \tag{4}$$

where $R(x)$ is the distance from the vertical Z-axis (of which the origin is at the front stagnation point) to the body surface. The appropriate boundary conditions are:

$$y=0:\ u=v=0;\quad T=T_w(x)=T_\infty+\Delta T_0\left(\frac{x}{L}\right)^p,$$

or

$$-k\frac{\partial T}{\partial y}=q_w(x)=q_0\left(\frac{x}{L}\right)^s, \tag{5}$$

$$y\to\infty:\ u=0;\quad T=T_\infty,$$

where L is the length of body, k is the thermal conductivity of the fluid, and p, s, and ΔT_0 are constants.

For most non-Newtonian fluids the Prandtl number is quite large, and thus the inertial effect of the flow, represented by the two terms on the LHS of equation (2), may be neglected [1]. Under this assumption, it can be readily shown that similarity solutions exist for the problem described by equations (1)–(5) in which the body shape of the 2-D body varies according to

$$\sin\varepsilon=(x/L)^m. \tag{6}$$

To study the two cases of surface thermal conditions prescribed by equation (5), we assign $i = 1$ for the case of variable wall-temperature and $i = 2$ for the case of variable wall-heat-flux in the following transformations:

$$\eta_i=c_iy_ix_i^{\lambda_i-1},\quad \psi_i=d_ix_i^{\lambda_i}f(\eta_i),\quad \theta_i=(T-T_\infty)/G_i, \tag{7}$$

where ψ is the stream function and

$$x_i=x/L,\quad y_i=H_iy/L,\quad c_i=\lambda_i^{nt_i},$$

$$d_i=\lambda_i^{-(2n+1)t_i},\quad t_i=1/(3n+i),$$

$$\lambda_1=(m+p+2n+1)t_i,\quad \lambda_2=(m+s+2n+2)t_2,$$

$$G_1=T_w-T_\infty,\quad G_2=c_2H_2k/(q_0L)x_2^{(m-n-3sn-s)t_2},$$

$$H_i=Gr_i^{0.5/(n/i+i)}\,Pr_i^{n/(3n+i)},$$

* Present address: RCA-Astro-Electronics Space Center, Princeton, NJ 08540, U.S.A.